Exploring the possibilities of identification and classification of excessive water addition in chicken breasts by spectral imaging

N.W. Kasander

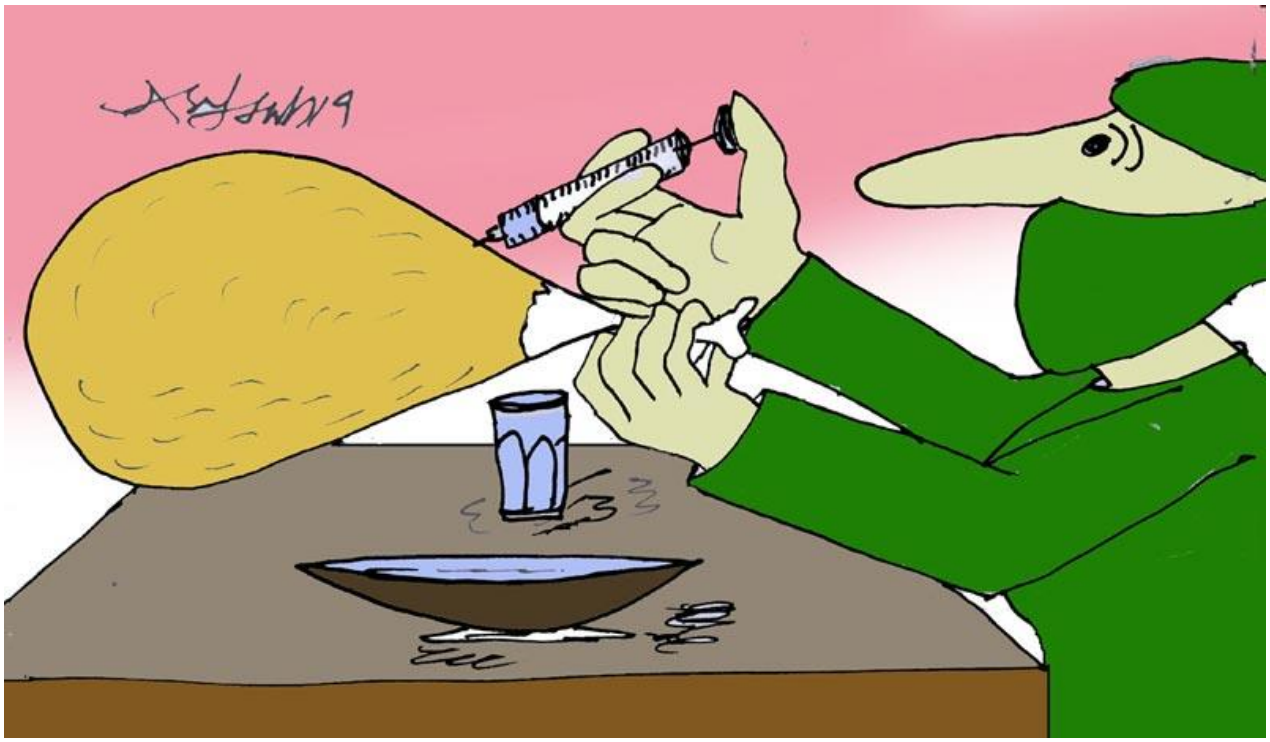

(Daily Times, 2019)

Wageningen University and Research
Department of Food Quality and Design

WAGENINGEN
UNIVERSITY & RESEARCH

Title: Exploring the possibilities of identification and classification of excessive water addition in chicken breasts by spectral imaging
By: Nikos William Kasander
Student number: 1019691
Date: January - Augustus 2024
Supervisors:
Dr. S.W. Erasmus
Dr. J.A. Peller
Wageningen University, FQD-80436

Abstract

In response to the conventional, time-consuming and chemical analysis for water detection in chicken, interest in quick, non-destructive methods have risen. The focus of this thesis is on the non-destructive method: spectral imaging. Hence, the aim of this study was to validate the possibilities of detecting fraud through excessive water addition by using a classification and prediction model utilising spectral and chemical data. With positive validation, this study can be used as a backbone for future research to optimize the prediction model for fraud detection. In this study, 36 chicken breasts were divided into three groups: a control (CO), a moderate water addition of 3-5% (MID) and a high water addition of 9-11% (HI). The breasts were imaged with SPECIM line scan spectral cameras and their water and protein contents were calculated by oven-drying and DUMAS respectively. The water/protein (w/p) ratios of the samples were calculated and a classification and prediction models were developed. The study revealed a good classification between the control and the treated groups, having correct identification of 78-92%. The classification between the two treatment groups was lower with correct identification values of 59-72%, which was expected as the moisture values of these breasts were in the end more similar than predicted. For the moisture prediction model, a partial least squares regression (PLSR) model was developed by using both the image and chemical data. For this, the most accurate model was determined by the lowest prediction residual errors sum of squares (PRESS), the highest R^2 and the variance. The highest variance was observed at 70%, which meant that the model could only predict the exact moisture content only 70% of the time. It is assumed that with a larger sample size, the accuracy of the model would increase as well. To conclude, this study validated the possibility of using spectral imaging for the detection of water addition fraud in chicken breast by positively recognising differences between different treatments and showing possibilities in accurately predicting the water content.

Preface and Acknowledgements

When I started my thesis in January, I was very excited about my research topic as I got the opportunity to adjust my topic based on my interest in food fraud. After the first year of my master's, I found out how much it amazed me that the average consumer knows so little about what they buy and consume, and that they lose trust in the food sector when fraud is committed. After this realisation, I was motivated to get to know more about this part of Food Technology and Food Safety and therefore also followed the course "Food Law". This course sparked my interest even more and I immediately looked for a thesis where I could pursue this. I was therefore very happy that Sara Erasmus and Joseph Peller gave me the opportunity to work on this exciting and promising field of research.

This thesis would not have been such an exciting and insightful project without the following people. Sara Erasmus, thank you for guiding me through the food related part of my thesis and giving extensive feedback. I learned a lot from this, and you inspired me to also want to explore this field further during my internship. Joseph Peller, thank you for helping me out with the spectral imaging machine as well as teaching me the basics of programming. This, I am very grateful for as it was always something that I wanted to learn. Thank you so much for your patience when things were not working as they were supposed to (often it was something like changing ":" into ";"). Seren Yigitturk I want to thank you for helping me out with answering my questions about the chicken samples and preparation. At last, I want to thank the lab technicians Erik Meulenbroeks and Jelle Bos for their help and explanations in the lab, as well as for the protein analysis and freeze-drying my samples. Something else I am thankful for are the thesis ring sessions as it was very insightful to see how other people delt with certain situations.

This thesis inspired me even more to pursue a career in the food fraud sector where I hope to contribute to tackling food fraud and making the food sector even more secure.

Table of contents

Abstract iii
Preface and Acknowledgements iv
List of abbreviations 1
1 Introduction 2
2 Materials and methods 5
2.1 Sample collection 6
2.2 Sample preparation 6
2.3 Spectral imaging and sample annotation 6
2.4 Moisture content 6
2.5 Protein content 7
2.6 Water/protein determination 7
2.7 Data analysis 8
2.7.1 Prediction model 8
2.7.2 Wavelength selection 8
2.7.3 Confusion matrix 8
3 Results and discussion 9
3.1 Spectral imaging 9
3.2 Moisture content 9
3.3 Protein content 10
3.4 Water/protein ratio 11
3.5 Confusion matrix 12
3.6 Image acquisition 14
3.7 Wavelengths selection 16
3.8 PLSR and Pearson correlation 18
4 Recommendations for future research 20
5 Conclusion 21
6 References 22
7 Appendix 24
7.1 Appendix A Moisture content 24
7.2 Appendix B Protein content 25

List of abbreviations

Abbreviations	Definition
CO	Control samples
EL	Elings
GF	Gert Driessen
HI	9-11% addition (highly treated) sample
HR	Hermsen
LVs	Latent variables
MID	3-5% addition (moderately treated) sample
NIR	Near-infrared
PCA	Principle component analysis
PLSR	Partial least squares regression
PRESS	Prediction residual errors sum of squares
ROI	Region of interest
SA	Natuuraslagerij Van Santen
W/p ratio	Water/protein ratio

1 Introduction

Chicken is a high-protein source of meat and a common food product in the human diet. Its quality has become of high importance to consumers and therefore more important for poultry farmers, producers and governmental control authorities as well (Ballin & Lametsch, 2008). The U.S. Department of Agriculture stated in 2023 that globally, with 33%, poultry is the second most widely consumed meat in the world (USDA, 2023). Due to the large demand and consumption of chicken and its high nutritional and market value, motivations may arise to look for opportunities to increase profit, especially taking into account that controlling bodies can lack in detecting fraud (Frankhuizen, et al., 2011). This makes chicken meat vulnerable to fraudulent practices within the supply chain (Lianou et al., 2021). Therefore, detecting and preventing food fraud in this sector as efficiently as possible is a must. Food fraud involves intentional modification of food products and associated documentation for economic gain and may lead to issues for food safety, legality and quality depending on the activities undertaken or the agents used. Food manufacturers, as part of the assessment of their vulnerability to food fraud, need to identify the individual food materials and products that they supply and produce that have a history of illegal activity (Manning & Soon, 2019).

In raw chicken breast meat, one of the most common ways of committing fraud is by adding excessive amounts of water (Ballin, 2010; Lianou et al., 2021). The official way to detect excessive water fraud is by calculating the water/protein (w/p) ratio. The current regulation states that the w/p ration may not exceed a value of 3.4 for chicken breasts (Commission Regulation (EC) No 543/2008 of 16 June 2008, 2008). The conventional way of determining this ratio is done by separately determining the water and protein contents with the use of recognised international organisation for standardisation (ISO) methods and other methods of analysis approved by the Council (Commission Regulation (EC) No 543/2008 of 16 June 2008, 2008). These methods are utilised to accurately analyse a single compound in food (Hussain et al., 2019). Problems with the current methods are that they are destructive, time-consuming and expensive (Cheng et al., 2013; Kharbach et al., 2023). For the analysis of excessive water addition, it was shown that these methods on their own were vulnerable to false negatives as well (Kharbach et al., 2023; Frankhuizen et al., 2011). A study by Frankuizen et al. (2011), showed this vulnerability as they experimented by applying the classical wet chemistry procedures on different treated chicken breast samples. The samples were treated with excessive amounts of water in combination with several different water-retaining agents. The study showed that the current analysis gave false negatives for ten samples as the methods could not distinguish between the chicken protein and the added protein which functioned as water retaining agent making it seem that the fraudulent samples had a legal w/p ratio. This showed that the current methods have flaws in identifying possible frauds while it is expensive and time-consuming. Next to this, it means that there are already possible methods that fraudsters can use to get away with the fraud they have committed. It is therefore essential that non-destructive methods should be explored which can be used as a rapid test to detect fraud. In case these non-destructive methods have similar accuracy compared to the conventional methods, these can be used to replace the current methods.

Therefore, it is necessary to research other methods which can analyse water and proteins. One of these methods is near-infrared (NIR) spectroscopy. NIR spectroscopy is a type of high-energy vibrational spectroscopy and analyses between the wavelength range from 400 to 1700 nm (Pasquini, 2018). NIR is a non-invasive and non-destructive method suitable for in-line use and minimal sample preparation is needed (Pasquini, 2003). The NIR spectral ranges occur mainly by exciting overtones, combinations and resonances of fundamental vibrational modes and are mostly associated with anharmonic vibrational modes of molecular functional groups containing C-H, O-H, N-H and S-H

(Weyer & LO, 2006). Next to this, vibrations of strong chemical bonds, such as a carbonyl group, can be detected by NIR spectroscopy as well (Pasquini, 2003, 2018).

As mentioned, NIR spectroscopy is rapid and non-destructive. In current literature, it has been shown that moisture and protein content could be determined by NIR-spectroscopy. However, to have qualitative and quantitative analysis, data mining and chemometrics are essentially required (Cheng et al., 2013). Next to this, NIR spectroscopy on its own lacks the visualisation of the whole product. To visualise the product, imaging is required. Imaging is the science and technology of acquiring spatial and temporal data information from objects. Another rapid, non-destructive method which combines spectroscopy and imaging is spectral imaging (Garini et al., 2006).

Spectral imaging has often been used for food products as a non-invasive analysis. Line-scan spectral imaging techniques have been intensively researched and developed for measuring the physical, chemical and biological properties of a broad range of foods and biological materials. The application scope has been expanded rapidly into many food and agricultural areas. The techniques have been intensively researched and developed with the use of different physical principles and wavelength ranges (Qin et al., 2017). Spectral imaging has been shown to measure the physical, chemical, and biological properties of food products for surface, subsurface and internal evaluations (Qin et al., 2017).

Spectral imaging has been used in several ways for the non-invasive analysis of properties in broiler chickens. It has been effectively used in combination with an algorithm for the inspection of wholesome chicken and systematically diseased chicken with accuracy and speed compared to human inspection (Chao et al., 2008; Yang et al., 2009). The freshness of chicken is an important aspect where fraud can be committed. An example of this is the detection of intact chicken breast muscle using NIR spectroscopy (Alexandrakis et al., 2012) where the researchers analysed the differences in reflectance of chicken breasts that were left for spoilage for 0, 4, 8 and 14 days. As it was known that NIR spectroscopy can analyse a possible increase of amides and amines, it was expected that protein hydrolysis would increase meaning that the differences in freshness could be analysed. Next to this, Xiong et al. (2015) studied the prediction of the Thiobarbituric acid reactive substances (TBARS) value of chicken meat for freshness evaluation. They analysed chicken meat during refrigerated storage with samples of 0, 3, 6, and 9 days old. He et al. (2023) determined the moisture content in chicken breasts by spectral imaging. In this study, the raw spectra were pre-processed and PLS models were constructed for the prediction of moisture, protein and ash. With the most optimal models, the moisture, protein and ash distributions were visualised.

Next to chicken, other meats have been analysed as well by using spectral imaging. Research has shown that properties like moisture content, proteins, and lipids can be analysed by spectral imaging (Barbin et al., 2015; Qin et al., 2017). Wang et al. (2017) determined the moisture content, of pork meat with the use of NIR-spectroscopy. The detection models used were based on a three-wavelength method, a partial least squares regression (PLSR) method, and a successive projection algorithm which allowed to select several featured wavelengths to reduce redundancy. For the moisture content analysis, three pieces of meat samples weighing around 5 grams were put in the oven at 105°C for 16 hours. The moisture content was calculated from the percentage weight loss (AOAC, 2005). ElMasry and Wold (2008) showed that the fat and moisture content of different fish species could be analysed by NIR spectrometry and PLSR. Next to this, ElMasry and Wold (2008) visually mapped the water and fat distribution as well, visualising it by a NIR imaging system. Another study on the quality properties of differently brined turkey hams was conducted which showed clear differences in reflection results with the different moisture contents (ElMasry et al., 2011). It hereby showed that an increase in

moisture content should be clearly visible and therefore it should be possible to detect fraud with the addition of water.

Research has been executed utilizing spectral imaging to assess the quality attributes of meat, such as water content, pH, fat and protein content. For fraud control in meat, adulteration, freshness, muscle discrimination and the farming system were tested (Mendez et al., 2019). Based on current literature, most experiments were conducted in processed meats, for example minced beef or sausages (McGrath et al., 2018; Mendez et al., 2019). Even though it has been shown that water can be detected with the use of spectral imaging, no literature was found on the detection of food fraud by excessive water addition by spectral imaging. Based on the found literature, it showed that spectral imaging is rapid, non-destructive, and it is possible to visualise water. In Annex VIII part A of the European regulation No 1169/2011 of the European Parliament and of the Council of 25 October 2011, it is stated that added water exceeding 5% of the total weight of the final product must be listed on the ingredient list. Therefore, this study aims to explore its possibilities to predict and detect food fraud by excessive water addition in chicken breast.

In this validation study, excessive water injection was visually mapped in intact chicken breasts using a calibrated prediction model of water and protein. These models were made with NIR spectroscopy and spectral imaging data of chicken breasts with determined water and protein contents.

This study aimed to validate the accuracy of the spectral imaging method in distinguishing between non-fraudulent and fraudulent chicken breasts. To achieve this aim, the following research questions and sub-questions are proposed:

To what extent can spectral imaging visually map and predict fraud by excessive water addition?

- How can spectral imaging distinguish between a legal and a fraudulent sample?
- To what extent can spectral imaging detect different concentrations of water in the chicken breast?
- How accurate will the PLSR and the classification models obtained from the spectral data be for the visual mapping and identification of the chicken samples**?**

Based on previous research, it was hypothesised that with spectral imaging combined with a well-designed model made with a large data set, it should be able to distinguish between fraudulent and non-fraudulent samples. Due to the limited data set, however, the accuracy of the model could be limited. The classification between different treated samples is expected to be accurate as the treated samples contain significantly more water compared to the non-treated control samples.

2 Materials and methods

The chicken breast samples were weighed and injected with a water solution according to their sample group and weight. Afterwards, the samples were imaged by spectral imaging to obtain the average spectra of each of the breasts. For quantitative data collection, the chicken breasts were prepared for both water and protein analysis. The acquired images were analysed and annotated with perClass Mira (perClass BV, Delft, Netherlands) and were exported to MATLAB (MathWorks, Massachusetts, United States) for classification and modelling of the moisture content. Figure 1A shows a flow chart with an overview of the whole experiment and Figure 1B shows a timeline of the whole experiment.

A

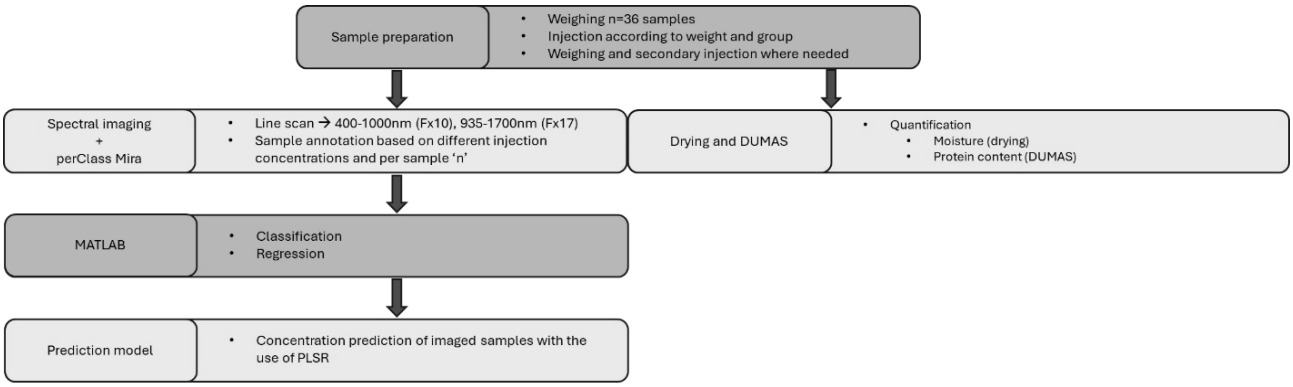

B

	Timeline																			
	Date																			
	March			April					May				June				July			
Project	11-15	18-22	25-29	01-05	08-12	15-19	22-26	29-03	06-10	13-17	20-24	27-31	03-07	10-14	17-21	24-28	01-05	08-12	15-19	22-26	29-02
Collecting samples																					
Spectral imaging																					
Homogenising samples																					
Moisture analysis																					
Protein analysis																					
Modelling																					

***Figure 1: Overview of the experiment containing the specific processes (1A) and timeline (1B**). The overview describes the processes of the sample preparation, spectral imaging, perClass Mira, drying, DUMAS, MATLAB, and the prediction model. The timeline ranges from March 2024-July 2024. In grey indicated is the timeline of the specific projects.*

2.1 Sample collection

A total of 36 chicken breast fillets were purchased from four different local butchers (nine breast fillets per butcher) located in Wageningen (two butchers) and Rhenen (two butchers), The Netherlands, to increase the variability of this research. Samples were purchased on 12/03/2024. The butchers were *Elings* (EL), *Natuurslagerij Van Santen* (SA), *Hermsen* (HR) and *Gert Driessen* (GF). On average, the weight of the individual chicken breasts was 200 g, except for the chicken breasts of GF, which were around 300 g per breast. The samples were divided into three groups with 12 (n) samples per group (three breasts per butcher): a control group of no water injection (CO), 3-5% of total weight gain in water addition (MID) and 9-11% of total weight gain in water addition (HI). A range of percentages was used for this experiment, as it was difficult to exactly inject the right percentage of solution. It was possible to use ranges, as this study is mainly for validation of spectral imaging being able to differentiate between fraudulent and non-fraudulent chicken breasts.

2.2 Sample preparation

The MID and HI samples were weighed before injection to determine the required injection volume. The injected solution comprised 92.5% water, 5% sodium-tripolyphosphate and 2.5% sodium chloride, to closely mirror realistic cases of fraud by water injection (Zheng et al., 1999). Samples were injected with the calculated amount of solution using a 5 mL and 10 mL syringe containing a 0.80 x 38mm needle. After injection, the samples were weighed again to ensure the lack of solution leakage. If this was the case, the samples were injected and weighed again until the sufficient weight was met. After spectral imaging, samples were prepared for moisture and protein content analyses. This was done by homogenising the samples according to AOAC Official Method 983.18 using a blender.

2.3 Spectral imaging and sample annotation

A line scan spectral imaging system containing FX10 and FX17 cameras (SPECIM, Oulu, Finland) was used. The system uses two LED bars and 500W halogen lamps (EFFILUX, Les Ulis, France) for scanning visible light and infrared light, respectively. A Teflon tile and closed shutter were applied for white and black calibration. The FX10 camera measures wavelengths between 400-1000 nm over 224 wavebands and FX17 measures wavelengths between 935-1700 nm over 112 wavebands. The obtained images consist of a 3D data structure where two dimensions are the spatial information and the last dimension stands for spectral information or number of wavelengths (I (x,y,λ)). The FX10 and FX17 images were acquired with waveband steps of 3 and 7 nm steps, respectively. The spectral image scanning was conducted nine times, having four samples per scan. All samples were first scanned with the FX10 camera and afterwards with the FX17.

After all samples were scanned, the images were annotated individually to determine the average spectrum per chicken breast. The annotating was done with perClass Mira which made it possible to further analyse the images. After annotation, the samples were exported to MATLAB for further analysis.

2.4 Moisture content

To determine the moisture content, an oven drying method was followed according to AOAC Official Method 934.01. First, the aluminium cricibles were dried and weight (w1). Afterwards, the samples were prepared in duplicate and weighed before and after drying (wt and w2 respectively). The moisture content was eventually calculated by subtracting both weights and the values were given in percentages of the sample:

$$Moisture\ (\%) = 100 - \frac{(w2 - w1)}{wt} * 100$$

2.5 Protein content

To determine the total protein content of the samples, a DUMAS method was used. With this method, the total N content was measured. With this obtained data and a nitrogen-to-protein conversion factor, the total amount of protein was determined. The samples were prepared by first freeze-drying the chicken breasts. Afterwards, the samples were ground into a fine powder, of which 5 mg were weighed in duplicate for the DUMAS analysis. After the DUMAS analysis, the nitrogen content of the samples was determined. The nitrogen values were multiplied with a conversion factor of 6.25 to obtain the percentage protein content of the dry weight (Pdw) (Hall & Schönfeldt, 2013). To calculate the percentage of protein of the total sample, the formula below was applied:

$$Protein\ (\%) = \big(100 - Moisture(\%)\big) * (\frac{Pdw(\%)}{100})$$

2.6 Water/protein determination

After calculating both the water and protein content, first, The moisture and protein values were averaged. After this, the water/protein (w/p) ratio could be calculated. This was done by taking the weights of the protein data and the known percentage of moisture for all samples. As the percentage of moisture was known, the percentage of dry matter was known as well. Using the dry matter percentage, the total weight was extrapolated from the known dried weight. Having these values, the total protein content and moisture content were calculated. These two values were then divided by each other to determine the w/p ratio. This gave the following formula:

$$Dry\ weight(\%) = 100 - Moisture(\%)$$

$$Total\ weight(mg) = \frac{Dry\ weight(mg)}{Dry\ weight(\%)} * 100$$

$$Dry, Moisture\ weight(mg) = Total\ weight(mg) * \frac{Dry\ weight, Moisture(\%)}{100}$$

$$w/p\ ratio = \frac{Moisture\ weight(mg)}{Dry\ weight(mg)} \leq 3.4$$

As mentioned, it is stated that the w/p ratio may not be more than 3.4. If the sample exceeds the value of 3.4, it is perceived as a non-legal sample.

2.7 Data analysis

2.7.1 Prediction model

For the prediction of the moisture content, a regression model was made. The regression model was made by applying partial least squares regression (PLSR). It compresses the spectral data into components called latent variables (LVs) which describe the maximum covariance between the spectral and experimental data (ElMasry, Sun, et al., 2011). It is therefore why PLSR is a good analysis for making prediction models of experimented data with specific wavelengths. Before performing PLSR, it is necessary to determine the number of LVs. To obtain an accurate model, high variance is required with limited LV to prevent overfitting of the model. Factors important for the determination of LVs are obtaining the lowest possible mean squared error (MSE) and the prediction residual errors sum of squares (PRESS) and the highest cumulative variation (ElMasry, Sun, et al., 2011; Wang et al., 2017).

This model can be used to visually map the prediction of the water and protein content. PLSR can be applied using the full spectra, however, by selecting the area with the most relevant wavelengths, the accuracy of the PLSR model can be improved (Osborne et al., 1997). As well as for the PCA analysis, the data was split into a training and test set to prevent overconfidence in regression (Barbin et al., 2015). The PLSR model was built with the training set and applied to the test set. The developed model was afterwards applied to the acquired images in perClass Mira.

2.7.2 Wavelength selection

To make the model as accurate as possible, a Pearson correlation analysis was conducted for this study to select specific key wavelengths. Pearson statistical correlation was used as this showed how two vectors are correlated. For both FX10 and FX17, the wavelength range of water will be used to observe which wavelengths specifically correlate the best. Negative values in Pearson correlation analysis mean that there is a negative correlation between the moisture values and the specific wavelengths (Homayouni & Roux, 2004; Mu et al., 2018). As the spectral imaging is in reflectance mode, a negative correlation means that there is a through at these specific wavelengths which then possibly corresponds to water in the samples.

2.7.3 Confusion matrix

To identify possible correlations between the samples a confusion matrix was developed. A confusion matrix provides an overview of how often a certain sample is detected correctly, and how often it is classified as another sample (Ruuska et al., 2018). First, the data was split into a training and a test set. Splitting the data is a widely used study design in high-dimensional settings. It divides the data as a means of estimating classification accuracy. This, in combination with a corresponding classifier developed on the training data and applied to the test data, helps make an accurate confusion matrix (Dobbin & Simon, 2011). Before making the correlation matrix a principal component analysis (PCA) was applied to lower the number of dimensions, enhancing the interpretability of the data while minimizing the data loss (Jolliffe & Cadima, 2016). It is important to find the right balance between the PCA value and the accuracy of the data. Having a too high PCA value would lead to an inaccurate read of the data. By trial and error, a suitable number of components were applied for the PCA. Combining both the splitting method with a PCA, made it possible to make an accurate confusion matrix. At last, a classifier is needed to make a confusion matrix. The classifier used for this study was least mean squares as this classifier gave the best classification with the least principal components.

3 Results and discussion

3.1 Spectral imaging

As mentioned, all samples were imaged by two cameras via spectral imaging. Figure 3 visualises two example images of the FX10 camera (A) and the FX17 camera (B), respectively. It is important to note that the last measurement of FX17 (CO3) was lost due to an unexpected broken lens which meant that this data could not be used for analysis. After annotation, the samples were saved and further analysed in MATLAB for model development.

3.2 Moisture content

As described before, the moisture content was determined by an oven-drying method. All samples were tested in duplicate. After obtaining the moisture data, the values were checked for non-realistic outliers by applying standard error and were repeated when necessary. The mean and standard deviation of all duplicate's moisture content are shown in Figure 1. After this repetition, all samples had realistic values. The moisture content values did not increase as much as expected, as the injection-treated samples only showed an increase of 1-2% moisture compared to the untreated control samples. This was unexpected as the treated samples were injected with 5% (MID) to 10% (HI). Potential reasons for lower moisture contents are that the samples were not able to retain the solution as expected. Besides, due to the leakage of all homogenised samples, it was possible that during the sampling, moisture was excreted and remained in the vacuum bags. This might have led to a lower moisture content from the taken samples than first envisioned. Appendix A provides a table containing all the moisture contents including the mean. For follow-up research, it is recommended to ensure no moisture is excreted from the homogenised chicken breasts. By properly mixing the samples before weighing, the moisture content determination becomes more accurate. Another and better option, is to analyse moisture with the fresh samples. Before moisture sampling, the samples were stored after injection, homogenised, frozen and defrosted. In between these steps, moisture loss can occur as well as a decrease in water-holding capacity (Oliveira et al., 2015).

Table 1: Average moisture content and standard deviation of samples obtained from the butchers Van Santen (SA), Hermsen (HR), Gert Driessen (GF) and Elings (EL). *The three treatment groups are: Control (CO), 3-5% moisture addition (MID) and 9-11% (HI).*

Sample	Moisture (%)	Std.dev	Sample	Moisture (%)	Std.dev
COSA1	73.34	0.422	COHR1	75.04	0.154
COSA2	73.93	0.148	COHR2	75.24	0.294
COSA3	74.71	0.013	COHR3	74.84	0.340
MIDSA1	74.83	0.333	MIDHR1	76.19	0.029
MIDSA2	74.85	0.367	MIDHR2	76.30	0.176
MIDSA3	75.40	0.207	MIDHR3	76.38	0.623
HISA1	75.90	0.067	HIHR1	76.55	0.166
HISA2	75.26	0.178	HIHR2	76.19	0.420
HISA3	76.64	0.216	HIHR3	76.58	0.223
Sample	Moisture (%)	Std.dev	Sample	Moisture (%)	Std.dev
COGF1	75.41	0.455	COEL1	73.60	0.154
COGF2	75.46	0.301	COEL2	73.67	0.347
COGF3	74.71	0.190	COEL3	73.82	0.086
MIDGF1	76.12	0.502	MIDEL1	74.06	0.080
MIDGF2	75.23	0.116	MIDEL2	74.61	0.185
MIDGF3	75.21	0.370	MIDEL3	74.36	0.144
HIGF1	75.47	0.293	HIEL1	75.46	0.313
HIGF2	77.44	0.120	HIEL2	75.87	0.004
HIGF3	77.32	0.025	HIEL3	75.30	0.421

3.3 Protein content

After the DUMAS test, the nitrogen content of the samples was determined. After this, the nitrogen values were multiplied with a conversion factor of 6.25 to obtain the protein content of the chicken samples (Hall & Schönfeldt, 2013) (Table 2). Samples MIDHR2 and HIHR2 were repeated as both samples were clear outliers compared to the other samples and there was a large difference between the duplicates. A possible reason for this was a manual weighing error which led to a higher observed protein content. After one repetition, both samples had an expected value. Besides the repeats, all samples were prepared on the same day to prevent variation as much as possible. At last, all duplicates were averaged to compare the different samples and were used to calculate the w/p ratio.

Table 2: Average Protein content and standard deviation of the dry weight of samples obtained from the butchers Van Santen (SA), Hermsen (HR), Gert Driessen (GF) and Elings (EL). *The three treatment groups are: Control (CO), 3-5% moisture addition (MID) and 9-11% (HI).*

Sample	Protein (%)	Std.dev.	Sample	Protein (%)	Std.dev.
COSA1	89.08	0.206	COHR1	91.08	0.542
COSA2	90.00	0.319	COHR2	89.40	0.216
COSA3	88.16	0.023	COHR3	87.87	0.186
MIDSA1	88.55	0.375	MIDHR1	86.21	0.461
MIDSA2	85.55	0.032	MIDHR2	85.40	0.260
MIDSA3	86.89	0.226	MIDHR3	87.36	0.033
HISA1	86.30	0.290	HIHR1	85.52	0.263
HISA2	86.61	0.344	HIHR2	81.91	0.148
HISA3	84.65	0.699	HIHR3	86.25	0.434
Sample	Protein (%)	Std.dev.	Sample	Protein (%)	Std.dev.
COGF1	86.95	0.090	COEL1	88.70	0.094
COGF2	85.99	0.124	COEL2	89.29	0.149
COGF3	84.23	0.051	COEL3	89.08	0.094
MIDGF1	82.95	0.086	MIDEL1	86.89	0.098
MIDGF2	82.48	0.190	MIDEL2	85.86	0.264
MIDGF3	83.38	0.190	MIDEL3	86.77	0.410
HIGF1	79.79	0.478	HIEL1	84.84	0.547
HIGF2	83.82	0.579	HIEL2	86.57	0.467
HIGF3	83.64	0.117	HIEL3	83.89	0.166

3.4 Water/protein ratio

After averaging all moisture and protein values, the w/p ratio was calculated. In Figure 2, all samples with the corresponding w/p ratio were visualised. The yellow-marked samples are samples exceeding the legal w/p value of 3.4. As expected, all HI samples exceeded the legal w/p ratio, as well as most of the MID samples. However, some MID samples did not exceed the value of 3.4. This was expected as the water addition of these samples barely exceeded the legal amount. Remarkably, the CO samples of "*Gert Driessen*" had an average w/p ratio between 3.5 and 3.6, exceeding the legal w/p ratio. One of the reasons for this value is that the butcher used an immersion chilling method to cool the chicken, or that there is a case of water addition of the chicken breasts. At last, important to note, is that the legal w/p ratio was determined 30 years ago. The natural w/p difference between chickens could have changed much compared to the chickens then, which would be the cause of a non-legal w/p ratio in the untreated samples without committing fraud (Elahi & Topping, 2012; Weesepoel et al., 2019). However, it was still remarkable to find that only all three control samples of one butcher exceeded the w/p ratio. To be sure, inspection and possible resampling could be a next step to find out more information about the non-legal w/p ratio.

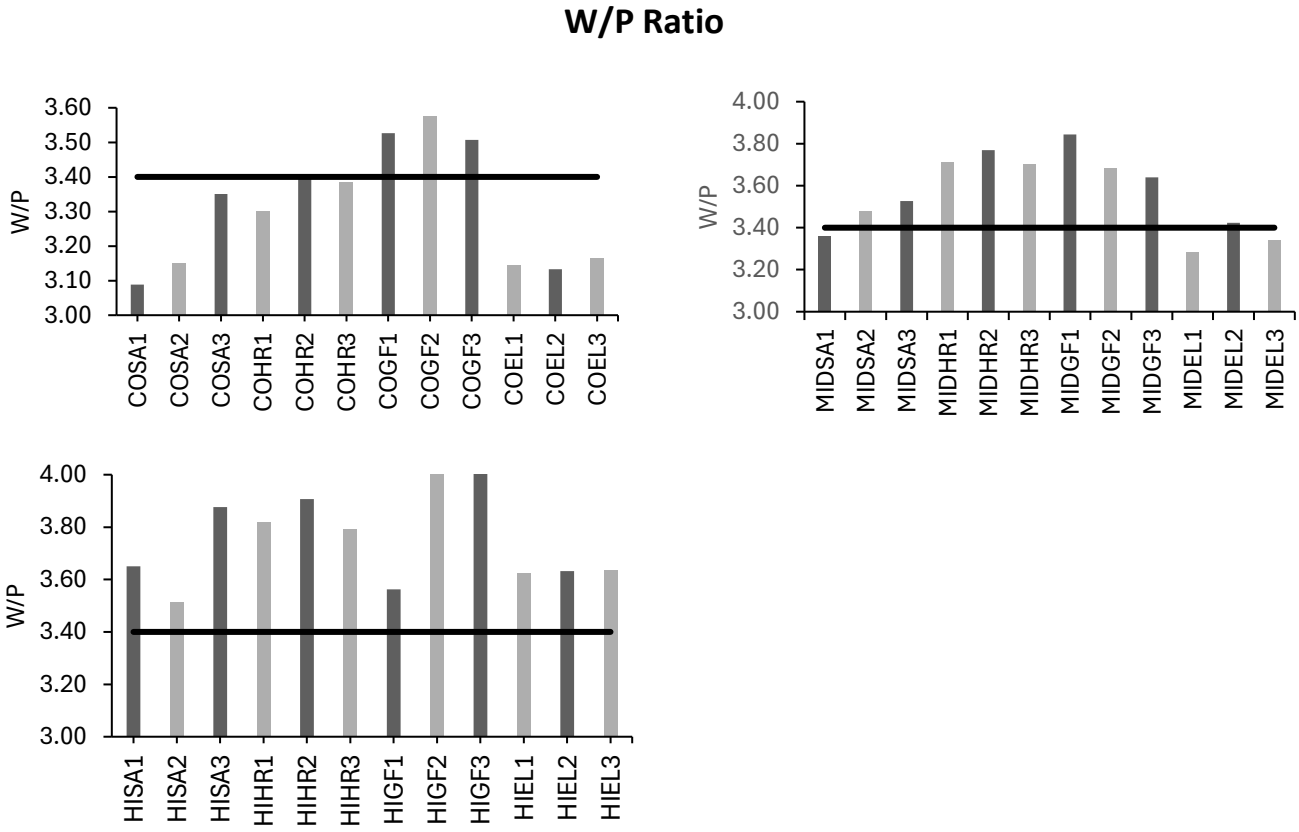

Figure 2: The water/protein ratio calculated with the obtained experimental data for all samples from the butchers Van Santen (SA), Hermsen (HR), Gert Driessen (GF) and Elings (EL), including a line = 3.4 to check if the samples exceed the legally allowed w/p limit. *The three treatment groups can be observed: Control (CO) (top left), 3-5% moisture addition (MID) (top right) and 9-11% (HI) (bottom left). If the values exceeded the line, they were considered to have a not legal ratio of water to protein.*

3.5 Confusion matrix

Confusion matrices were developed to observe the correct identification and comparison of the samples between the different butchers with the same treatment and between the different treatments. Both these comparisons were applied to the FX10 and FX17 data. In Tables 3 and 4 the confusion matrices were given for both the complete spectral data and the selected spectral data between 900 and 1000 nm and 935 and 1250 nm for FX10 and FX17, respectively. Due to the memory space of MATLAB, the comparison between treatments was split up into three different matrices: HI-CO, HI-MID, and MID-CO. The data can be read as how much of the data was perceived as its own group and how much of the data is confused with the data of another group. The total of these values always equals to one. For example, in Table 4, the table of Fx10 CO-MID showed that data 0.79 (79%) of CO was perceived correctly and that 0.21 (21%) of the data was confused with the MID sample group.

For this study, the number of principal components was set at ten, as this resulted in the lowest confusion with the least amount of components and the least mean squares were used as a classifier. It was expected that the samples from different butchers with the same treatment would not be identified correctly as the samples would have similar spectra. This meant that these groups were more likely to be confused with each other due to the fact that the chicken breasts had the same treatment and that the samples of different butchers were expected to have a similar chemical composition. The analysis confirmed most of these expectations, as there was no clear identification of the different sample groups. However, in Table 3 was observed that the identification tended to identify most groups with the 'GF' samples instead of their own group. Next to this, the 'GF' samples had the highest identification ratio compared to all groups, while the 'SA' group had the lowest identification ratio of the groups. The explanation of random values was explained by the similar spectra of the groups which are shown in section 3.6.

The identification between different treatments was expected to accurate as the reflectance of water should be different between the treatments, especially when the wavelengths for water were used. In Table 3, it can be observed that for both the FX17 and FX10 results, the samples were identified correctly for at least 78% when comparing the CO samples with the treated MID and HI samples. This was expected as the treated samples contained significantly more water than the control samples (CO). Nevertheless, the MID and HI samples were seemingly more difficult to identify from each other with correct identification between 61% and 72% accuracy, respectively. This was explained by the water addition in the samples of HI and MID being expressed in percentage ranges, where the highest percentage values of the MID samples could have been close to the low percentage addition of the HI samples. To conclude, this confusion matrix analysis contributed by confirming observed differences in the samples, resulting in the possibility of further analysis.

Table 4: The confusion matrices analysing the different treatments for both the FX10 (left) and FX17 (right) spectral images of the samples obtained from the butchers Van Santen (SA), Hermsen (HR), Gert Driessen (GF) and Elings (EL). *There were three treatment groups: Control (CO), 3-5% moisture addition (MID) and 9-11% (HI).*

			Fx10		
Sample	COSA	COHR	COGF	COEL	Total
COSA	0.002	0.354	0.625	0.018	1
COHR	0.002	0.567	0.395	0.036	1
COGF	0.001	0.175	0.804	0.017	1
COEL	0.001	0.117	0.846	0.037	1

			Fx17		
Sample	COSA	COHR	COGF	COEL	Total
COSA	0.011	0.366	0.443	0	1
COHR	0.02	0.47	0.344	0	1
COGF	0.001	0.117	0.752	0	1
COEL	0.02	0.023	0.39	1	1

Sample	MIDSA	MIDHR	MIDGF	MIDEL	Total
MIDSA	0.048	0.407	0.312	0.234	1
MIDHR	0.032	0.317	0.415	0.201	1
MIDGF	0.015	0.289	0.53	0.166	1
MIDEL	0.04	0.27	0.374	0.316	1

Sample	MIDSA	MIDHR	MIDGF	MIDEL	Total
MIDSA	0.15	0.273	0.347	0	1
MIDHR	0.0057	0.377	0.422	0	1
MIDGF	0.041	0.322	0.467	0	1
MIDEL	0.065	0.166	0.355	0	1

Sample	HISA	HIHR	HIGF	HIEL	Total
HISA	0.264	0.118	0.53	0.088	1
HIHR	0.186	0.355	0.38	0.079	1
HIGF	0.161	0.14	0.607	0.092	1
HIEL	0.126	0.187	0.617	0.071	1

Sample	HISA	HIHR	HIGF	HIEL	Total
HISA	0.001	0.112	0.778	0	1
HIHR	0.001	0.465	0.444	0	1
HIGF	0.001	0.179	0.673	0	1
HIEL	0.003	0.169	0.627	0	1

Table 5: The confusion matrices analysing the treatment groups Control (CO), 3-5% Moisture addition (MID) and 9-11% moisture addition (HI) for both FX10 (left) and FX17 (right) spectral images.

		Fx10	
Group	CO	MID	Total
CO	0.79	0.21	1
MID	0.237	0.763	1
Group	CO	HI	Total
CO	0.785	0.215	1
HI	0.18	0.82	1
Group	MID	HI	Total
MID	0.614	0.386	1
HI	0.273	0.727	1

		Fx17	
Group	CO	MID	Total
CO	0.783	0.217	1
MID	0.098	0.902	1
Group	CO	HI	Total
CO	0.827	0.173	1
HI	0.075	0.925	1
Group	MID	HI	Total
MID	0.59	0.41	1
HI	0.327	0.673	1

3.6 Image acquisition

Figure 3 shows a typical spectral image of both the FX10 (A) and FX17 (B) cameras where the region of interest (ROI) was already annotated. The typical spectra obtained from these images are shown in Figure 4. As can be observed, the FX10 spectra showed very few obvious peaks and throughs. It was important to observe these throughs as every through in these spectra corresponded to a chemical component like for example water or protein. Not having clear throughs and peaks might be due to possible overlapping noise in this wavelength range of 400-940 nm. The only clear trough observed was at wavelengths between the range of 940-1000 nm. The spectra of FX17 showed clear peaks and troughs at the wavelength range between 935-1250 nm and limited reflectance was observed in the wavelength range between 1300-1700 nm as the signal around these wavelengths was not as strong. The overlapping troughs of 940-1000 nm FX10 and 935-1250 nm of FX17 spectra matched with one of the absorption wavelengths of water.

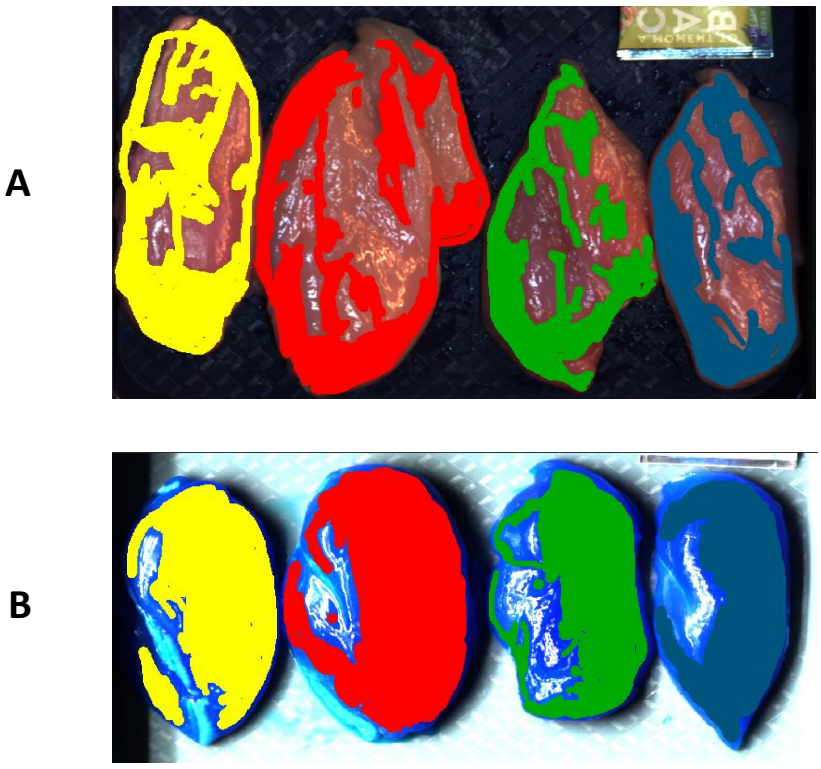

Figure 3: Image acquisition and annotation of images from the (A) FX10 camera and the (B) FX17 camera*. The colours blue, green, red and yellow correspond to the butchers Van Santen (SA), Hermsen (HR), Gert Driessen (GF) and Elings (EL)*

A

B

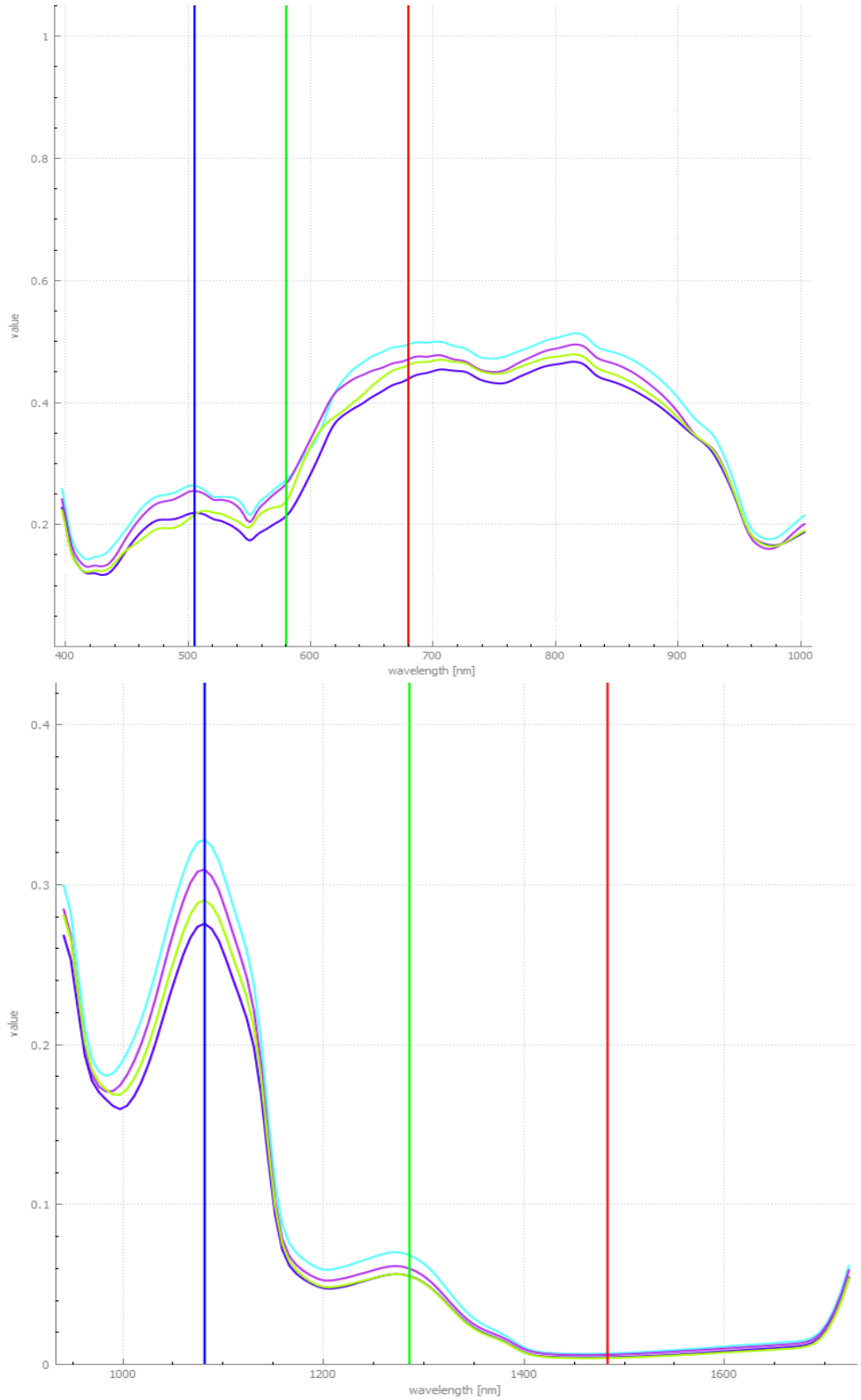

Figure 4: Average spectrum of the chicken samples obtained from the (A) FX10 camera and the (B) FX17 camera. *The light blue, lilac, light green and purple spectra correspond to the butchers Gert Driessen (GF), Van Santen (SA), Elings (EL) and Hermsen (HR) respectively.*

3.7 Wavelengths selection

The prediction model was expected to become more accurate when only a selection of wavelengths was used compared to the full spectra. For selecting the wavelength range, the absorption spectrum of water was used as a reference, as in Figure 5. In the Figure, absorbance peaks can be observed at around 5000 cm^{-1} (2000 nm), 7000 cm^{-1} (1429 nm) and between 9500 and 11000 cm^{-1} (909 and 1050 nm) For this research, the small peak between 9500 and 11000 cm^{-1} (909-1050 nm) was used as this was the only peak within the imaged spectrum (Afrin et al., 2013). Afrin et al., 2013 stated that this peak corresponded to "$2v_1 + v_3$", which meant a two times symmetrical stretch and one asymmetrical stretch of O-H (Afrin et al., 2013; Buijs & Choppin, 1963; Carleer et al., 1999). Meat studies of ElMasry et al. 2011 and Yang et al. 2018 first determined the optimal wavelength selection by the use of PCA and plotting the wavelengths against the eigenvectors, and using established regression coefficients from PLSR respectively. With this, both studies obtained wavelengths corresponding to the wavebands of water found from literature (ElMasry, et al., 2011; Yang et al., 2018). As was observed in Figure 4(A) and (B), expected throughs were located at the mentioned wavelength range. This range of wavelengths was therefore selected to create the PLSR prediction model. As mentioned, for a specific wavelength selection, a Pearson correlation analysis was conducted for this study. For both FX10 and FX17, the wavelength range of water was used to observe which wavelengths specifically correlated the best (Figure 6). The graphs showed clear troughs at the expected wavelengths which corresponded to the absorbance spectrum of water as absorbance is perceived as a trough in reflectance analysis. For comparison, both the wavelength range and the selected wavelengths were used to make a PLSR model to compare the accuracy.

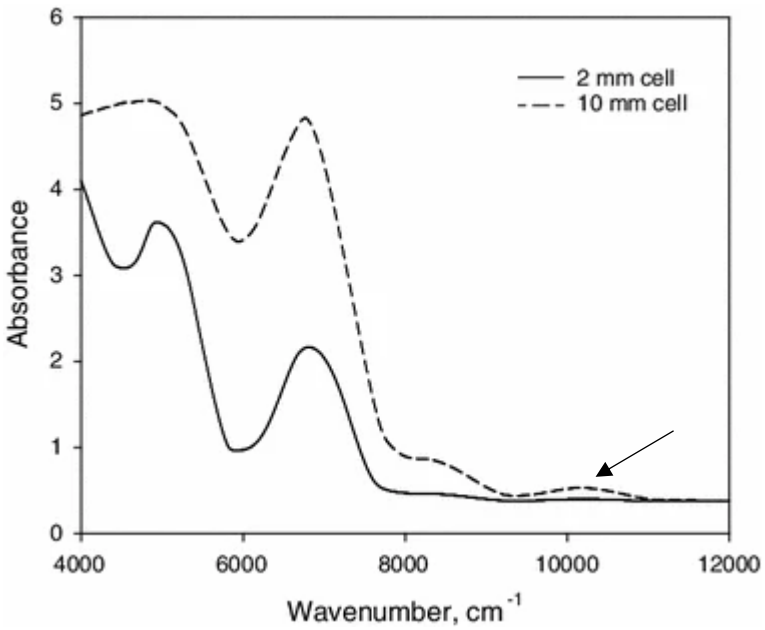

Figure 5: Two examples of the absorption spectrum of water. On the X-axis the wavenumber was given (1/wavelength) (Afrin et al.,2013). *The arrow indicates the absorbance peak used for this study.*

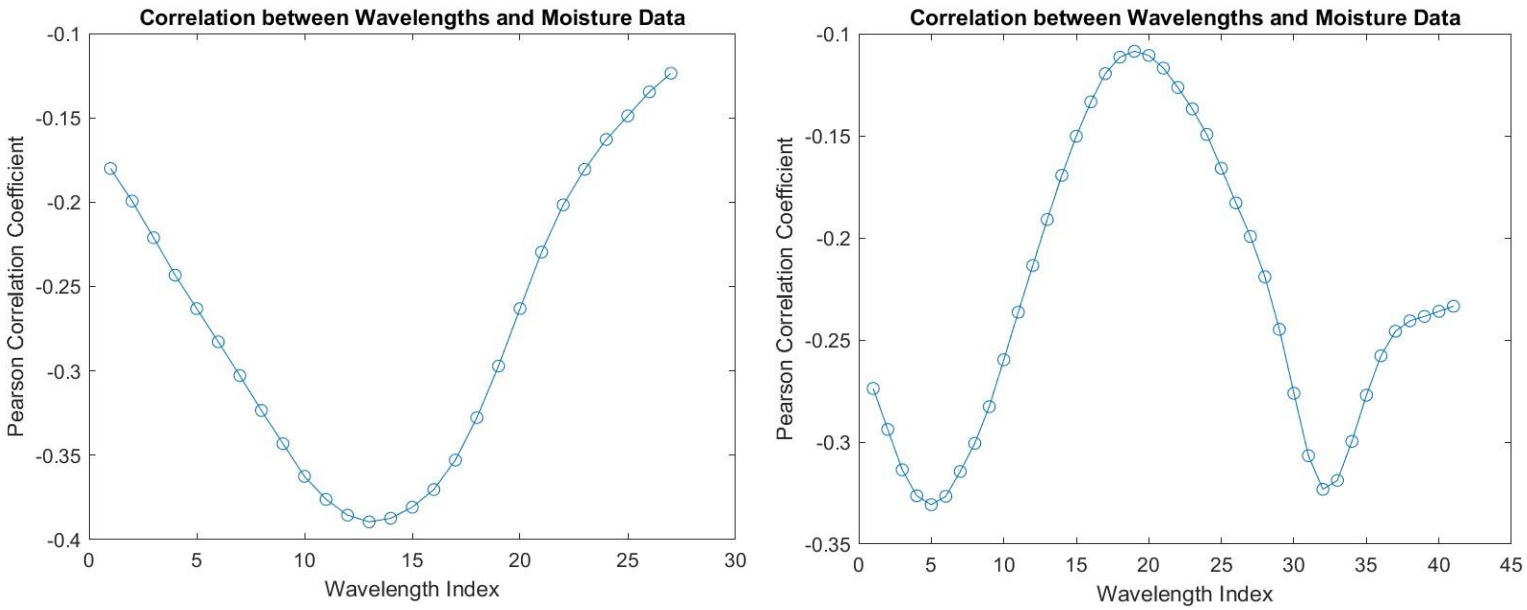

Figure 6: Pearson correlation graphs acquired from the (left) FX10 and the (right) FX17. *The troughs observed in both graphs correspond to the absorption peaks of water and the corresponding wavelengths were therefore selected for modelling.*

3.8 PLSR and Pearson correlation

After image acquisition and annotation, and determining the moisture and protein contents, a PLSR model was developed. A model for the selected wavelength range was developed.

First, the spectral data containing spectra of more than 300000 points was averaged which gave only one value per specific waveband. After that, just as for the confusion matrix, the dataset was split into a training and test set with a ratio of 0.7 and 0.3 respectively. As mentioned, the accuracy and reproducibility were determined by the factors MSE, the PRESS and R^2. Table 6 shows the wavelength selection obtained from the water spectra and the Pearson correlation analysis with their corresponding factors. The specific wavelengths showed to have the lowest PRESS and MSE for both FX10 and FX17, validating that the selected wavelengths make a more accurate model for the moisture analysis. The maximum variance corresponding to the least amount of LVs however, did not exceed more than 70%.

To test if the accuracy of the model was accurate enough to find differences between fraudulent and non-fraudulent samples, regression models were made (Figure 7). The scattered values of both Figures showed that the predicted values differed at most 1% of the actual moisture content. During the moisture content and the w/p ratio analysis, it was observed that 1% difference in moisture could make a big difference in the w/p ratio. This would mean that with this model, some chicken breasts can be tested false positive and false negative. However, the inaccuracy of this model could be due to the small sample size. Follow-up research is recommended to increase the sample size of the chicken breasts, as well as obtain the chicken from more different sources to increase the variation in samples as well.

Table 6: The different wavelength selections with their corresponding factors (PRESS, MSE, R^2) for both FX10 and FX17.

FX10

Wavelengths	PRESS	MSE	R2
930.36-1024.11 (25)	7.085	3.449	0.704
949.11-975.89 (11)	x	1.584	0.640

FX17

Wavelengths	PRESS	MSE	R2
948.11-1186.79 (35)	8.713	2.796	0.820
948.11, 955.13, 962.15, 969.17, 976.19, 983.21, 990.23, 997.25, 1004.27, 1151.69, 1158.71, 1165.73, 1172.75, 1179.77, 1186.79 (15)	5.592	1.191	0.831

A

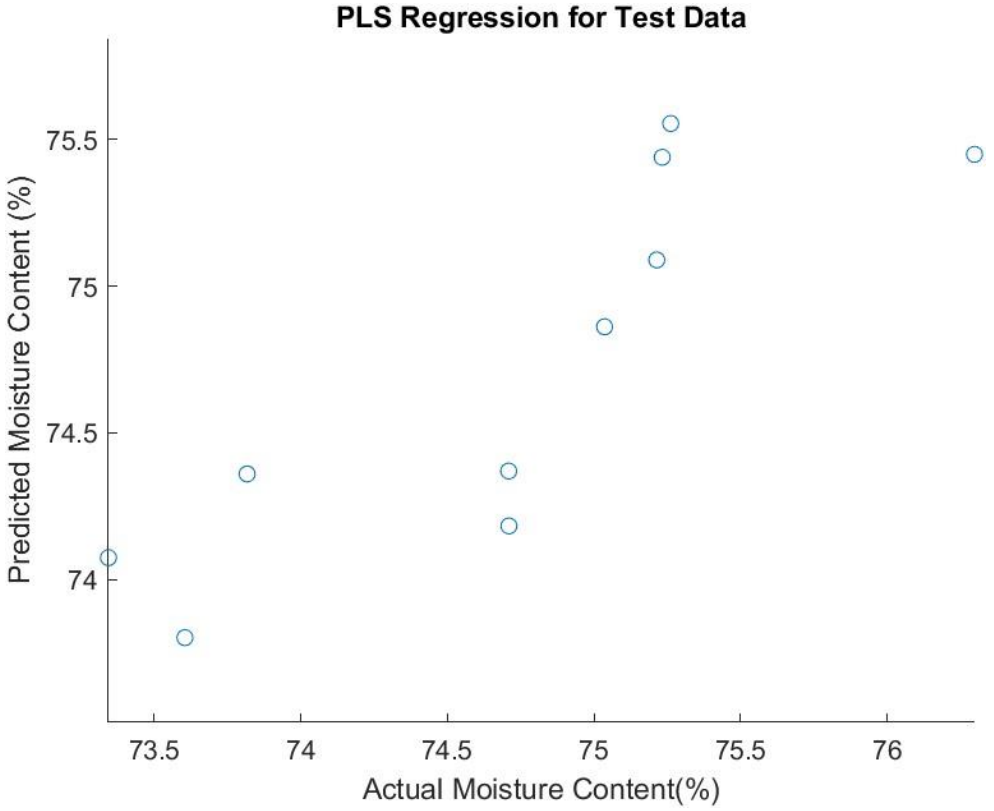

B

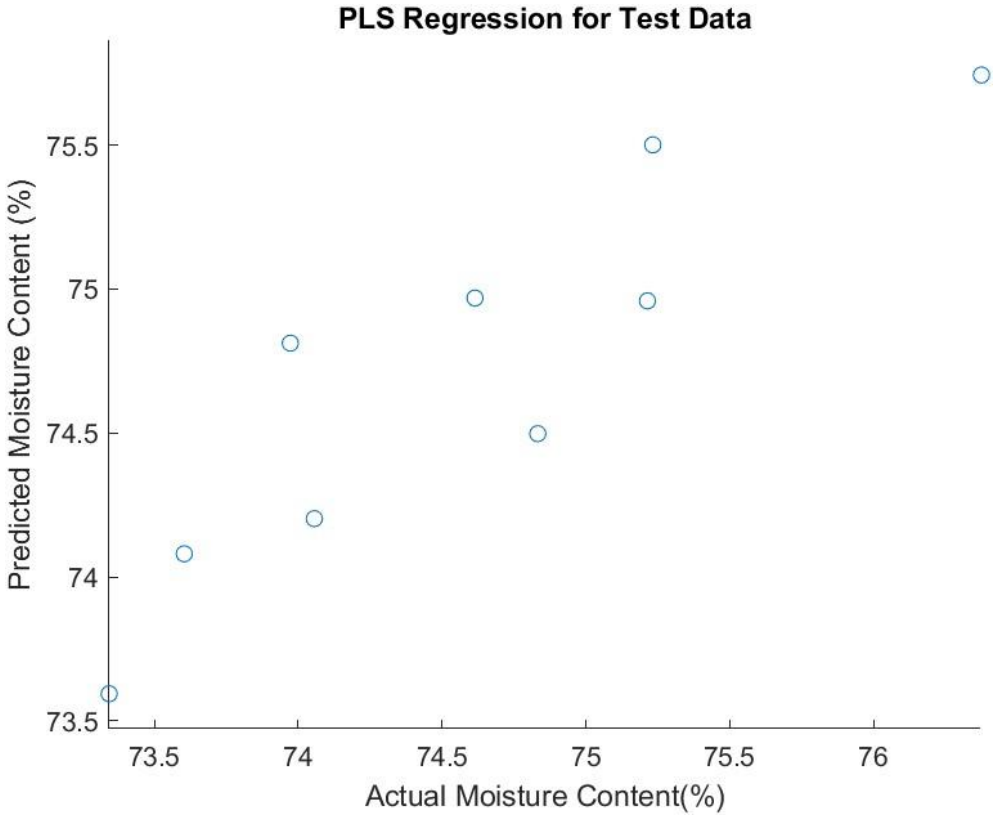

Figure 7: PLS regression models applied on the test set of n=9 for both Fx10 data (A) and Fx17 data (B).

4 Recommendations for future research

For future research, it is recommended to increase the accuracy of both the model and data by using a larger dataset and obtain samples from more varying sources to increase the variation of the data as well. Besides having a large dataset, it is recommended to study the possibilities of making a visual map for the protein as well in the hope of fully using spectral imaging instead of chemical analysis. Having both the accurately predicted value for water and protein would make it possible to calculate the w/p ratio without the use of chemical analysis, making spectral imaging a possible new method for detecting excessive water in chicken breasts as well as other meats At last, the time between analyses should be minimalized. In this study, the chicken breasts were homogenised and analysed when they were three weeks old. If further research shows that models can be made accurate enough, it is aimed to apply spectral imaging in practise and replace the conventional way of testing chicken breasts.

5 Conclusion

This study aimed to find out to what extent spectral imaging could be used to visually map and predict excessive water addition, and how accurate a PLSR and classification model were to identify chicken samples with different treatments. First, the PLSR models obtained from the spectral and experimented moisture data of the chicken showed promising results, as the model was at most 1% off the actual measured moisture content. This is a promising result as this small sample size validated the possibility to make a map of the moisture content. Next to this, confusion matrices showed clear classification and identification of different treated sample groups around the water absorbance region. Hereby validating the possibility to observe clear differences between the fraudulent and control samples. Due to the small dataset, no definite conclusion could be made. However, these results showed the possibility of using spectral imaging data to be able to visually map and classify fraudulent injected chicken samples after more extensive research, with the hope that in the future, spectral imaging can replace the conventional methods of detection.

6 References

Afrin, T., Karobi, S. N., Rahman, M. M., Mollah, M. Y. A., & Susan, Md. A. B. H. (2013). Water Structure Modification by Sugars and Its Consequence on Micellization Behavior of Cetyltrimethylammonium Bromide in Aqueous Solution. *Journal of Solution Chemistry*, *42*(7), 1488–1499. https://doi.org/10.1007/s10953-013-0050-6

Alexandrakis, D., Downey, G., & Scannell, A. G. M. (2012). Rapid Non-destructive Detection of Spoilage of Intact Chicken Breast Muscle Using Near-infrared and Fourier Transform Mid-infrared Spectroscopy and Multivariate Statistics. *Food and Bioprocess Technology*, *5*(1), 338–347. https://doi.org/10.1007/s11947-009-0298-4

AOAC, C. (2005). Official Methods of Analysis of the Association of Analytical Chemists International. *Official Methods: Gaithersburg, MD, USA*.

Ballin, N. Z. (2010). Authentication of Meat and Meat Products. *Meat Science*, *86*(3), 577–587. https://doi.org/10.1016/j.meatsci.2010.06.001

Ballin, N. Z., & Lametsch, R. (2008). Analytical Methods for Authentication of Fresh vs. Thawed meat – A Review. *Meat Science*, *80*(2), 151–158. https://doi.org/10.1016/j.meatsci.2007.12.024

Barbin, D. F., Kaminishikawahara, C. M., Soares, A. L., Mizubuti, I. Y., Grespan, M., Shimokomaki, M., & Hirooka, E. Y. (2015). Prediction of Chicken Quality Attributes by Near-infrared Spectroscopy. *Food Chemistry*, *168*, 554–560. https://doi.org/10.1016/j.foodchem.2014.07.101

Buijs, K., & Choppin, G. R. (1963). Near-Infrared Studies of the Structure of Water. I. Pure Water. *The Journal of Chemical Physics*, *39*(8), 2035–2041. https://doi.org/10.1063/1.1734579

Carleer, M., Jenouvrier, A., Vandaele, A.-C., Bernath, P. F., Mérienne, M. F., Colin, R., Zobov, N. F., Polyansky, O. L., Tennyson, J., & Savin, V. A. (1999). The Near-infrared, Visible, and Near-ultraviolet Overtone Spectrum of Water. *The Journal of Chemical Physics*, *111*(6), 2444–2450. https://doi.org/10.1063/1.479859

Chao, K., Yang, C.-C., S. Kim, M., & E. Chan, D. (2008). High Throughput Spectral Imaging System for Wholesomeness Inspection of Chicken. *Applied Engineering in Agriculture*, *24*(4), 475–485. https://doi.org/10.13031/2013.25135

Cheng, J.-H., Dai, Q., Sun, D.-W., Zeng, X.-A., Liu, D., & Pu, H.-B. (2013). Applications of Non-destructive Spectroscopic Techniques for Fish Quality and Safety Evaluation and Inspection. *Trends in Food Science & Technology*, *34*(1), 18–31. https://doi.org/10.1016/j.tifs.2013.08.005

Commission Regulation (EC) No 543/2008 of 16 June 2008, 157 OJ L (2008). http://data.europa.eu/eli/reg/2008/543/oj/eng

Daily Times. (2019, November 19). Water-injected Chicken. *Daily Times*. https://dailytimes.com.pk/503139/water-injected-chicken/

Dobbin, K. K., & Simon, R. M. (2011). Optimally Splitting Cases for Training and Testing High Dimensional Classifiers. *BMC Medical Genomics*, *4*(1), 31. https://doi.org/10.1186/1755-8794-4-31

Elahi, S., & Topping, J. (2012). *Study of Physiological Water Content of Poultry Reared in the EU*. LGC. https://op.europa.eu/en/publication-detail/-/publication/62d443c3-ce7c-4fbe-962c-7ec06f9d95a3

ElMasry, G., Iqbal, A., Sun, D.-W., Allen, P., & Ward, P. (2011). Quality Classification of Cooked, Sliced Turkey Hams using NIR Hyperspectral Imaging System. *Journal of Food Engineering*, *103*(3), 333–344. https://doi.org/10.1016/j.jfoodeng.2010.10.031

ElMasry, G., Sun, D.-W., & Allen, P. (2011). Non-destructive Determination of Water-holding Capacity in Fresh Beef by Using NIR Hyperspectral Imaging. *Food Research International*, *44*(9), 2624–2633. https://doi.org/10.1016/j.foodres.2011.05.001

ElMasry, G., & Wold, J. P. (2008). High-Speed Assessment of Fat and Water Content Distribution in Fish Fillets Using Online Imaging Spectroscopy. *Journal of Agricultural and Food Chemistry*, *56*(17), 7672–7677. https://doi.org/10.1021/jf801074s

Frankhuizen, Bollen, M., & van Ruth, S. (2011). *Extraneous Water in Import Poultry Meat: Detection with EU Regulatory and Additional Tools*. https://edepot.wur.nl/178128

Garini, Y., Young, I. T., & McNamara, G. (2006). Spectral imaging: Principles and Applications. *Cytometry Part A*, *69A*(8), 735–747. https://doi.org/10.1002/cyto.a.20311

Hall, N. G., & Schönfeldt, H. C. (2013). Total Nitrogen vs. Amino-acid Profile as Indicator of Protein Content of Beef. *9th International Food Data Conference: Food Composition and Sustainable Diets*, *140*(3), 608–612. https://doi.org/10.1016/j.foodchem.2012.08.046

He, H.-J., Wang, Y., Ou, X., Ma, H., Liu, H., & Yan, J. (2023). Rapid Determination of Chemical Compositions in Chicken Flesh by Mining Hyperspectral Data. *Journal of Food Composition and Analysis*, *116*, 105069. https://doi.org/10.1016/j.jfca.2022.105069

Homayouni, S., & Roux, M. (2004). *Hyperspectral Image Analysis for Material Mapping Using Spectral Matching*. *20*, 28.

Hussain, N., Sun, D.-W., & Pu, H. (2019). Classical and Emerging Non-destructive Technologies for Safety and Quality Evaluation of Cereals: A Review of Recent Applications. *Trends in Food Science & Technology*, *91*, 598–608. https://doi.org/10.1016/j.tifs.2019.07.018

Jolliffe, I. T., & Cadima, J. (2016). Principal Component Analysis: A Review and Recent Developments. *Philosophical Transactions of the Royal Society A: Mathematical, Physical and Engineering Sciences*, *374*(2065), 20150202. https://doi.org/10.1098/rsta.2015.0202

Kharbach, M., Alaoui Mansouri, M., Taabouz, M., & Yu, H. (2023). Current Application of Advancing Spectroscopy Techniques in Food Analysis: Data Handling with Chemometric Approaches. *Foods*, *12*(14), Article 14. https://doi.org/10.3390/foods12142753

Lianou, A., Papakonstantinou, M., Nychas, G.-J. E., & Stoitsis, J. (2021). Chapter 6—Fraud in Meat and Poultry products. In R. S. Hellberg, K. Everstine, & S. A. Sklare (Eds.), *Food Fraud* (pp. 85–108). Academic Press. https://doi.org/10.1016/B978-0-12-817242-1.00012-9

Manning, L., & Soon, J. M. (2019). Food Fraud Vulnerability Assessment: Reliable Data Sources and Effective Assessment Approaches. *Trends in Food Science & Technology*, *91*, 159–168. https://doi.org/10.1016/j.tifs.2019.07.007

McGrath, T. F., Haughey, S. A., Patterson, J., Fauhl-Hassek, C., Donarski, J., Alewijn, M., van Ruth, S., & Elliott, C. T. (2018). What are the Scientific Challenges in moving from Targeted to Non-targeted Methods for Food Fraud Testing and how can they be Addressed? – Spectroscopy case study. *Trends in Food Science & Technology*, *76*, 38–55. https://doi.org/10.1016/j.tifs.2018.04.001

Mendez, J., Mendoza, L., Cruz-Tirado, J. P., Quevedo, R., & Siche, R. (2019). Trends in Application of NIR and Hyperspectral Imaging for Food Authentication. *Scientia Agropecuaria*, *10*(1), 143–161. https://doi.org/10.17268/sci.agropecu.2018.01.16

Mu, Y., Liu, X., & Wang, L. (2018). A Pearson's Correlation Coefficient Based Decision Tree and its Parallel Implementation. *Information Sciences*, *435*, 40–58. https://doi.org/10.1016/j.ins.2017.12.059

Oliveira, M. R., Gubert, G., Roman, S. S., Kempka, A. P., & Prestes, R. C. (2015). Meat Quality of Chicken Breast Subjected to Different Thawing Methods. *Brazilian Journal of Poultry Science*, *17*, 165–171. https://doi.org/10.1590/1516-635x1702165-172

Osborne, S. D., Künnemeyer, R., Osborne, S. D., & Jordan, R. B. (1997). Method of Wavelength Selection for Partial Least Squares. *The Analyst*, *122*(12), 1531–1537. https://doi.org/10.1039/a703235h

Pasquini, C. (2003). Near Infrared Spectroscopy: Fundamentals, Practical Aspects and Analytical Applications. *Journal of the Brazilian Chemical Society*, *14*, 198–219. https://doi.org/10.1590/S0103-50532003000200006

Pasquini, C. (2018). Near infrared spectroscopy: A Mature Analytical Technique with New Perspectives – A review. *Analytica Chimica Acta*, *1026*, 8–36. https://doi.org/10.1016/j.aca.2018.04.004

Qin, J., Kim, M. S., Chao, K., Chan, D. E., Delwiche, S. R., & Cho, B.-K. (2017). Line-Scan Hyperspectral Imaging Techniques for Food Safety and Quality Applications. *Applied Sciences*, *7*(2). https://doi.org/10.3390/app7020125

Ruuska, S., Hämäläinen, W., Kajava, S., Mughal, M., Matilainen, P., & Mononen, J. (2018). Evaluation of the Confusion Matrix Method in the Validation of an Automated System for Measuring Feeding Behaviour of Cattle. *Behavioural Processes*, *148*, 56–62. https://doi.org/10.1016/j.beproc.2018.01.004

USDA. (2023). *What is the Most Consumed Meat in the World?* https://ask.usda.gov/s/article/What-is-the-most-consumed-meat-in-the-world

Wang, J.-X., Fan, L.-F., Wang, H.-H., Zhao, P.-F., Li, H., Wang, Z.-Y., & Huang, L. (2017). Determination of the Moisture Content of Fresh Meat Using Visible and Near-Infrared Spatially Resolved Reflectance Spectroscopy. *Biosystems Engineering*, *162*, 40–56. https://doi.org/10.1016/j.biosystemseng.2017.07.004

Weesepoel, Y., Silletti, E., Alewijn, M., & Bernreuther, A. (2019). Importance of Harmonised Sample Preparation for Moisture and Protein Content Determinations in Official Food Control Laboratories: A Poultry Meat Case Study. *Food Chemistry*, *301*, 125291. https://doi.org/10.1016/j.foodchem.2019.125291

Weyer & LO. (2006). *Spectra–Structure Correlations in the Near-infrared*. https://www.s-a-s.org/assets/docs/0470027320_Spectra%E2%80%93_Structure_Correlations_in_the_Near%E2%80%90Infrared.pdf

Yang, C.-C., Chao, K., & Kim, M. S. (2009). Machine Vision System for Online Inspection of Freshly Slaughtered Chickens. *Sensing and Instrumentation for Food Quality and Safety*, *3*(1), 70–80. https://doi.org/10.1007/s11694-008-9067-8

Yang, Y., Wang, W., Zhuang, H., Yoon, S.-C., & Jiang, H. (2018). Fusion of Spectra and Texture Data of Hyperspectral Imaging for the Prediction of the Water-Holding Capacity of Fresh Chicken Breast Filets. *Applied Sciences*, *8*(4), Article 4. https://doi.org/10.3390/app8040640

Zheng, M., Toledo, R., & Wicker, L. (1999). Effect of Phosphate and Pectin on Quality and Shelf-Life of Marinated Chicken Breast. *Journal of Food Quality*, *22*(5), 553–564. https://doi.org/10.1111/j.1745-4557.1999.tb00186.x

7 Appendix

7.1 Appendix A Moisture content

Table 7: The moisture data of all samples in duplicate and mean obtained via the drying method. *Every table shows the moisture data of samples originating from the same butcher: SA (top left), HR (top right), GF (bottom left) and EL (bottom right). The three treatment groups can be observed: Control (CO), 3-5% moisture addition (MID) and 9-11% (HI).*

Sample	Moisture conc. (%)	Mean (%)	Sample	Moisture conc. (%)	Mean (%)
COSA 1.1	73.04	73.34	COHR 1.1	74.93	75.04
COSA 1.2	73.64		COHR 1.2	75.14	
COSA 2.1	73.82	73.93	COHR 2.1	75.44	75.24
COSA 2.2	74.03		COHR 2.2	75.03	
COSA 3.1	74.70	74.71	COHR 3.1	75.08	74.84
COSA 3.2	74.72		COHR 3.2	74.60	
MIDSA 1.1	75.07	74.83	MIDHR 1.1	76.17	76.19
MIDSA 1.2	74.60		MIDHR 1.2	76.21	
MIDSA 2.1	74.59	74.85	MIDHR 2.1	76.42	76.30
MIDSA 2.2	75.11		MIDHR 2.2	76.17	
MIDSA 3.1	75.25	75.40	MIDHR 3.1	76.82	76.38
MIDSA 3.2	75.54		MIDHR 3.2	75.93	
HISA 1.1	75.95	75.90	HIHR 1.1	76.67	76.55
HISA 1.2	75.86		HIHR 1.2	76.43	
HISA 2.1	75.14	75.26	HIHR 2.1	76.49	76.19
HISA 2.2	75.39		HIHR 2.2	75.90	
HISA 3.1	76.80	76.64	HIHR 3.1	76.42	76.58
HISA 3.2	76.49		HIHR 3.2	76.73	

Sample	Moisture conc. (%)	Mean (%)	Sample	Moisture conc. (%)	Mean (%)
COGF 1.1	75.73	75.41	COEL 1.1	73.71	73.60
COGF 1.2	75.09		COEL 1.2	73.50	
COGF 2.1	75.25	75.46	COEL 2.1	73.42	73.67
COGF 2.2	75.68		COEL 2.2	73.91	
COGF 3.1	74.58	74.71	COEL 3.1	73.76	73.82
COGF 3.2	74.84		COEL 3.2	73.88	
MIDGF 1.1	75.77	76.12	MIDEL 1.1	74.11	74.06
MIDGF 1.2	76.48		MIDEL 1.2	74.00	
MIDGF 2.1	75.32	75.23	MIDEL 2.1	74.75	74.61
MIDGF 2.2	75.15		MIDEL 2.2	74.48	
MIDGF 3.1	74.95	75.21	MIDEL 3.1	74.26	74.36
MIDGF 3.2	75.48		MIDEL 3.2	74.46	
HIGF 1.1	75.68	75.47	HIEL 1.1	75.24	75.46
HIGF 1.2	75.27		HIEL 1.2	75.68	
HIGF 2.1	77.35	77.44	HIEL 2.1	75.87	75.87
HIGF 2.2	77.52		HIEL 2.2	75.87	
HIGF 3.1	77.34	77.32	HIEL 3.1	75.60	75.30
HIGF 3.2	77.30		HIEL 3.2	75.00	

7.2 Appendix B Protein content

Table 8: The protein data of the dry weight of all samples in duplicate obtained via DUMAS. *Every table shows the protein data of samples originating from the same butcher: SA (top left), HR (top right), GF (bottom left) and EL (bottom right). The three treatment groups can be observed: Control (CO), 3-5% moisture addition (MID) and 9-11% (HI).*

Sample	Protein (%)	Mean (%)	Sample	Protein (%)	Mean (%)
COSA 1.1	89.23	89.08	COHR 1.1	91.20	91.58
COSA 1.2	88.94		COHR 1.2	91.96	
COSA 2.1	89.78	90.00	COHR 2.1	89.56	89.40
COSA 2.2	90.23		COHR 2.2	89.25	
COSA 3.1	88.18	88.16	COHR 3.1	87.74	87.87
COSA 3.2	88.15		COHR 3.2	88.00	
MIDSA 1.1	88.28	88.55	MIDHR 1.1	86.53	86.21
MIDSA 1.2	88.81		MIDHR 1.2	85.88	
MIDSA 2.1	85.57	85.55	MIDHR 2.1	85.22	85.40
MIDSA 2.2	85.52		MIDHR 2.2	85.58	
MIDSA 3.1	87.05	86.89	MIDHR 3.1	87.38	87.36
MIDSA 3.2	86.73		MIDHR 3.2	87.34	
HISA 1.1	86.09	86.30	HIHR 1.1	85.33	85.52
HISA 1.2	86.50		HIHR 1.2	85.70	
HISA 2.1	86.85	86.61	HIHR 2.1	81.81	81.91
HISA 2.2	86.37		HIHR 2.2	82.02	
HISA 3.1	85.14	84.65	HIHR 3.1	86.56	86.25
HISA 3.2	84.15		HIHR 3.2	85.94	

Sample	Protein (%)	Mean (%)	Sample	Protein (%)	Mean (%)
COGF 1.1	87.02	86.95	COEL 1.1	88.82	88.70
COGF 1.2	86.89		COEL 1.2	88.58	
COGF 2.1	86.08	85.99	COEL 2.1	89.19	89.29
COGF 2.2	85.91		COEL 2.2	89.40	
COGF 3.1	84.20	84.23	COEL 3.1	89.01	89.08
COGF 3.2	84.27		COEL 3.2	89.14	
MIDGF 1.1	82.89	82.95	MIDEL 1.1	86.96	86.89
MIDGF 1.2	83.01		MIDEL 1.2	86.82	
MIDGF 2.1	82.30	82.48	MIDEL 2.1	86.05	85.86
MIDGF 2.2	82.66		MIDEL 2.2	85.68	
MIDGF 3.1	83.51	83.38	MIDEL 3.1	86.48	86.77
MIDGF 3.2	83.24		MIDEL 3.2	87.06	
HIGF 1.1	80.13	79.79	HIEL 1.1	84.46	84.84
HIGF 1.2	79.45		HIEL 1.2	85.23	
HIGF 2.1	84.23	83.82	HIEL 2.1	86.90	86.57
HIGF 2.2	83.41		HIEL 2.2	86.24	
HIGF 3.1	83.72	83.64	HIEL 3.1	84.01	83.89
HIGF 3.2	83.56		HIEL 3.2	83.77	